American Mineralogist, Volume 89, pages 610–613, 2004

The crystal structure of painite $CaZrB[Al_9O_{18}]$ revisited

THOMAS ARMBRUSTER,[1,*] NICOLA DÖBELIN,[1] ADOLF PERETTI,[2] DETLEF GÜNTHER,[3] ERIC REUSSER,[4] AND BERNARD GROBÉTY[5]

[1]Laboratorium für chemische mineralogische Kristallographie, University of Bern, Freiestrasse 3, CH-3012 Bern, Switzerland
[2]GRS Gemresearch Swisslab Ltd., Hirschmattstrasse 6, CH-6003 Luzern, Switzerland
[3]Laboratory of Inorganic Chemistry—Elemental and Trace Analysis ETH Hönggerberg, HCI, G113, CH-8093 Zürich, Switzerland
[4]Institute of Mineralogy and Petrography, Sonneggstrasse, 5 ETH Zentrum, CH-8092 Zürich, Switzerland
[5]Department of Geosciences, University of Fribourg, Pérolles, CH-1700 Fribourg, Switzerland

ABSTRACT

The crystal structure of the rare hexagonal mineral painite [a = 8.724(1), c = 8.464(2) Å] from Mogok (Myanmar), with the ideal composition $CaZrB[Al_9O_{18}]$, was re-determined by single-crystal X-ray diffraction. Structure refinements were performed in space groups $P6_3/m$ and $P6_3$. The centrosymmetric $P6_3/m$ model yielded excellent agreement (R_1 = 1.44%, 1189 reflections > 2σ I_{obs}, 54 parameters) with the observed diffraction data without any unusual atomic displacement parameters, thus the acentric $P6_3$ model was rejected. A previous structural study claimed that painite was non-centrosymmetric and differed from the related structures of jeremejevite $B_5[\square_3Al_6(OH)_3O_{15}]$ and fluoborite $B_3[Mg_9(F,OH)_9O_9]$ in having lower symmetry.

The structure of painite comprises a framework of AlO_6 octahedra that features two types of channels parallel to the **c** axis. One channel has a trigonal cross-section and is occupied by threefold coordinated B and Zr in sixfold prismatic coordination. The other channel has a hexagonal cross-section and is occupied by Ca. Chemical analysis by laser-ablation inductively-coupled plasma-mass spectrometry indicated that the crystal studied has significant substitution of Na for Ca (ca. 20%) charge-balanced by Ti^{4+} replacing octahedral Al leading to the formula $Ca_{0.77}Na_{0.19}Al_{8.80}Ti_{0.19}Cr_{0.03}V_{0.01}Zr_{0.94}Hf_{0.01}B_{1.06}O_{18}$.

INTRODUCTION

Painite was first described by Claringbull-Gordon et al. (1957) and is still one of the world's rarest collector gemstones (Webster 1994). The mineral was found in the Mogok Stone Tract and was named after Arthur Charles Davy Pain who was a well-known mineralogist and gemologist of the area. Painite is so rare that the available specimens are individually numbered. Samples are currently deposited in the collection of the Natural History Museum in London (crystals no. 1 and no. 2). Crystal no. 3 is in the collection of the Gemological Institute of America. Crystal no. 4 is now in two pieces; both are privately owned. One small slice from sample no. 1 is at the California Institute of Technology. Recently two more samples have been discovered by A. Peretti. A 2.54 ct faceted sample was identified through testing in the GRS Gemresearch laboratory in Bangkok (Thailand) and is labeled painite no. 5 (world's largest gem-quality faceted sample). Painite no. 6a, a large rough fragment of 54 cts (dimensions: 18.7 × 14.3 × 10.8 mm), was discovered during an expedition (Peretti 2003) in May 2002 to Mogok close to the type locality, the private, government-licensed Ohn-Gaing mine at Sagaing. A small fragment (0.15 ct) of this rough painite was labeled painite no. 6b. The data presented in this paper were obtained from painite nos. 5 (chemistry) and 6b (chemistry and structure), whereas the large mother piece remained in Mogok.

The type locality for painite is located in the Mogok Belt of marbles and schists. This is also the origin of all hitherto reported specimens. The original Proterozoic sediments were regionally metamorphosed during the Cretaceous collision of the Burma block, a Godwana fragment, and later (Eocene) with the Indian plate. Granitic and syenitic intrusions and associated pegmatites are responsible for the contact metamorphic and metasomatic overprint found in some of the rocks (Iyer 1953; Harlow 2000). The alluvial deposits around the mining site contain minerals characteristic of the surrounding marbles and pegmatites such as ruby, sapphire, red spinel, pyrite, blue moonstone (oligoclase), red and brown zircons, and large black tourmaline crystals. Painite no. 6a was overgrown by ruby.

The crystal structure of painite was determined by Moore and Araki (1976), who describe it as a hexagonal [a = 8.715(2), c = 8.472(2) Å], rigid, and dense octahedral framework with space group $P6_3$, deviating slightly from the centrosymmetric space group $P6_3/m$. Initially, Moore and Araki (1976) assumed space group $P6_3/m$ but a corresponding refinement converged at R = 16% yielding unexpectedly large displacement parameters for the Al sites (B_{eq} = 1.5–3 Å^2). This was taken as evidence that the structure was in fact non-centrosymmetric and a subsequent refinement in space group $P6_3$ converged at 7.1% leading to reasonable isotropic displacement parameters for the Al sites. Furthermore, Moore and Araki (1976) speculated that the related structure of jeremejevite $Al_6(BO_3)_5F_3$ will also reveal space group $P6_3$ in future state-of-the-art structure refinements. Since Golovastikov et al. (1955) new structure refinements of jeremejevite have been published by Sokolova et al. (1987) and Rodellas et

* E-mail: thomas.armbruster@krist.unibe.ch

al. (1983) yielding $P6_3/m$ symmetry without any indication of deviation from centrosymmetry. Thus the symmetry problem of painite needed to be revisited. It is also important to note that the question of non-centrosymmetry or centrosymmetry has important bearings on the physical properties of a material.

Experimental methods

Major, minor, and trace element concentrations were measured by electron microprobe analysis (cut stone no. 5) and laser-ablation inductively coupled plasma-mass spectrometry (LA-ICP-MS; no. 5 and fragment no. 6b). The electron-microprobe (EMP) analyses were done with a CAMECA SX-100 instrument using natural oxides as standards. The only minor element detected was titanium. The following trace elements have concentrations close to the detection limit of the system: Cr, Hf, and Sc. No rare earth elements were detected. The electron microprobe analyses were used to normalize the LA-ICP-MS measurements (Table 1).

The LA-ICP-MS system consists of a 193 nm ArF excimer laser (GeoLasC, MicroLas, Göttingen, Germany) coupled to an ICP-mass spectrometer (Elan 6100, Perkin Elmer, Norwalk, U.S.A.) (Günther et al. 1997). The reference material NIST 612 was used as external calibration standard and Al was used as an internal standard (ablation and drift correction). Transient signal evaluation was carried out using the protocol described by Longerich et al. (1996). Each sample was analyzed 5 times using a spatial resolution of 60 μm (Table 1). Following Shigley et al. (1986), we analyzed (Table 1) several species in minor and trace amounts: Cr, V, and Hf, some of which – namely Cr^{3+} and V^{3+}—responsible for the red-orange color of painite.

The refractive indices of painite were determined with a conventional refractometer and a Brewster-angle refractometer. The latter instrument was necessary because the highest refractive index is greater than 1.81. The optical character was confirmed to be uniaxial negative using a polariscope and projection sphere for painite no. 5 and by immersion microcopy for sample 6b. Both crystals show strong pleochroism from brownish-red to orange-yellow. The Brewster angles for painites nos. 5 and 6a were measured as 60.1(1)°, 61.1(1)°, and 60.5(1)°, 61.1(1)°, respectively. The refractive indices for no. 5 are $\varepsilon = 1.789$ (measured with a conventional refractometer) and $\omega = 1.815$ (calculated from Brewster angle measurements). High birefringence was confirmed by microscopic investigations (facet and inclusion doubling). In spite of the increased Na and Ti content of the sample used (Table 1) the measured refractive indices are not significantly different from literature data for painite with less or no Na and Ti (Shigley et al. 1986). Sample no. 5 showed strong greenish-blue fluorescence under short wave UV light. The density of samples nos. 5 and 6b were determined hydrostatically yielding 4.00(1) g/cm^3.

The structure of a fragment (200 × 200 × 500 μm in diameter) of painite crystal no. 6b was studied by single-crystal X-ray diffraction with an Enraf-Nonius CAD4 diffractometer with graphite-monochromated Mo$K\alpha$ X-radiation at 293 K. Data reduction, including background and Lorentz polarization corrections, and an empirical absorption correction based on ψ scans, were performed using the SDP program library (Enraf-Nonius 1983). Single-crystal structure refinements using the program SHELX-97 (Sheldrick 1997) were done in space groups $P6_3$ and $P6_3/m$. However, the excellent resultant R_1 value of 1.44% for space group $P6_3$/m without any indication of unusual anisotropic displacement parameters led to rejection of the $P6_3$ model. Site occupancy refinements clearly indicated that the electron density at the Ca site is significantly below 20 e/Å^3 as expected for complete Ca occupancy. In our refinement we fixed the population of both Zr and B to full occupancy to cope with strong correlations of the atomic displacement parameter of Zr with the overall scale factor, and to reduce the number of refined parameters. Parameters related to the data collection and the structure refinement are listed in Table 2. Atomic coordinates and isotropic displacement parameters (B_{eq}) are shown in Table 3. Anisostropic displacement parameters are summarized in Table 4.

Table 1. LA-ICP-MS analyses of painite

Sample	No. 5	No. 6b
(wt%)		
CaO	6.81	6.34
Na_2O	0.46	0.87
Al_2O_3	66.03	66.03
TiO_2	1.69	2.26
B_2O_3	5.23	5.46
ZrO_2	16.89	17.02
HfO_2	0.32	0.29
V_2O_3	0.09	0.16
Cr_2O_3	0.05	0.31
Total	97.57	98.74
(apfu)		
Ca	0.84	0.77
Na	0.10	0.19
Al	8.92	8.80
Ti	0.15	0.19
B	1.03	1.06
Zr	0.94	0.94
Hf	0.01	0.01
V	0.01	0.01
Cr	0.01	0.03
Total cations	12.01	12.00
Ca + Na	0.94	0.96

Discussion

Initial test refinements in space group $P6_3$ led to strong correlations among sites related by centrosymmetry, and the accuracy of the model could be dramatically improved by refinement in space group $P6_3/m$ converging at $R_1 = 1.44\%$ without any indication of unusual displacement parameters for any position. This is clear evidence that at least the painite crystal studied by us is in fact centrosymmetric.

The framework of painite is composed of edge-sharing bands of AlO_6 octahedra extending along [001] which are laterally linked by shared edges and corners. The painite structure (Fig. 1) features two types of channels parallel to the **c** axis. The

Table 2. Data collection and refinement parameters for painite

crystal size (mm)	0.2 × 0.2 × 0.5
refined composition	$Ca_{0.93}ZrB[Al_9O_{18}]$
space group	$P6_3/m$
a (Å)	8.724(1)
c (Å)	8.464(2)
θ max. (°)	40
hkl (min., max.)	$-15 \le h \le 13$
	$0 \le k \le 15$
	$-15 \le l \le 15$
scan type	1.0° ω + 0.35 tan θ
Measured reflections	7221
observed reflections [$I > 2\sigma(I)$]	1189
unique reflections	1209
number of parameters	54
R_{int} (%)	1.95
R_1 (%)	1.44
wR_2 (%)	3.45
GooF	1.407

Table 3. Positional parameters and B_{eq} (Å^2) with standard deviations in parentheses for painite

Atom	x	y	z	B_{eq} (Å^2)
Zr	2/3	1/3	1/4	0.277(1)
Ca (Na)	0	0	0	1.148(6)
Al1	0.34290(2)	0.36082(3)	0.07794(2)	0.314(2)
Al2	0.33656(4)	0.00426(3)	1/4	0.344(3)
O1	0.88145(6)	0.40477(6)	0.09293(5)	0.381(4)
O2	0.19303(6)	–0.10735(6)	0.08217(5)	0.405(5)
O3	–0.11034(8)	–0.32921(8)	1/4	0.474(7)
O4	0.44764(8)	–0.15362(8)	1/4	0.452(7)
B	1/3	–1/3	1/4	0.41(1)

Table 4. Anisotropic displacement parameters with standard deviations in parentheses for painite

atom	U_{11}	U_{22}	U_{33}	U_{12}	U_{13}	U_{23}
Zr	0.00342(4)	0.00342(4)	0.00368(5)	0.00171(2)	0	0
Ca	0.0059(1)	0.0059(1)	0.0318(2)	0.00295(5)	0	0
Al1	0.00351(7)	0.00449(7)	0.00386(8)	0.00194(5)	0.00000(5)	0.00045(5)
Al2	0.00400(9)	0.00418(9)	0.0042(1)	0.00151(7)	0	0
O1	0.0049(1)	0.0046(1)	0.0050(1)	0.0023(1)	0.0005(1)	0.0002(1)
O2	0.0047(1)	0.0047(1)	0.0050(1)	0.0016(1)	–0.0002(1)	0.0000(1)
O3	0.0055(2)	0.0090(2)	0.0048(2)	0.0046(2)	0	0
O4	0.0050(2)	0.0039(2)	0.0077(2)	0.0019(2)	0	0
B	0.0048(3)	0.0048(3)	0.0061(5)	0.0024(1)	0	0

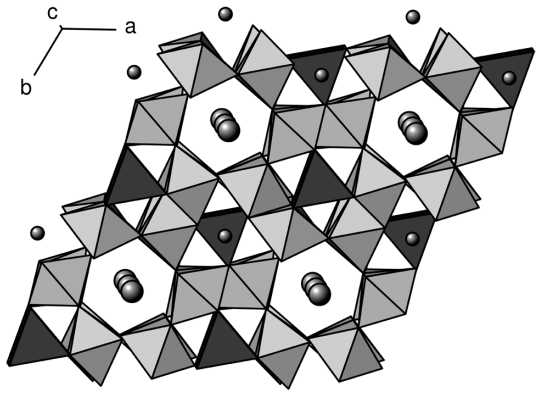

FIGURE 1. The structure of painite is composed of corner- and edge sharing AlO_6 octahedra. The hexagonal channels contain Ca^{2+} cations (large spheres), whereas the six-membered triangular channels contain B^{3+} (small spheres) and Zr^{4+} atoms. The dark triangles represent the relatively rare triangular-prismatic coordination of Zr by O atoms. Ca^{2+} can also be regarded as the central atom of a strongly distorted Ca-O octahedron.

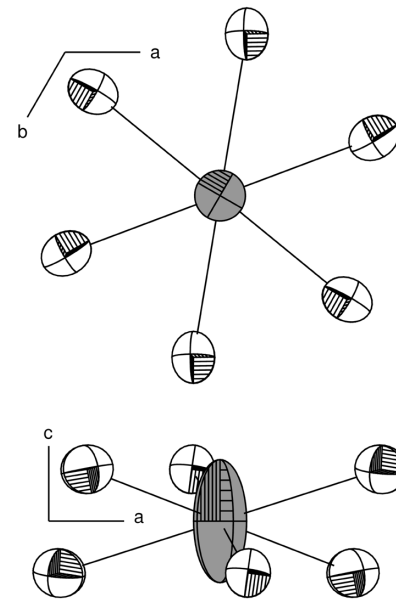

FIGURE 2. The Ca^{2+} site is located at 0, 0, 0 and lies on the 6_3 screw axis. It is surrounded by six symmetrically equivalent O2 sites at an almost ideal bonding distance (Ca-O2 = 2.403 Å). This arrangement can either be regarded as an extremely distorted octahedron, or as a distorted hexagon. The central cation is relatively free to move parallel to the **c** axis, which is reflected in the strongly anisotropic atomic displacement parameters (probability ellipsoids are arbitrarily scaled for better illustration).

larger channel, at the origin, has a hexagonal cross-section and is occupied by Ca^{2+} at $z = 0$ and 0.5, whereas the second type, located at 1/3, 2/3, z, has a triangular cross-section and contains B^{3+} at $z = 0.25$ and Zr^{4+} at $z = 0.75$, respectively. The Zr^{4+} site is coordinated by six symmetry equivalent O1 sites, which are related by the threefold axis and the perpendicular mirror plane, leading to trigonal prismatic arrangement. The bonding distance (2.121 Å) corresponds to the ideal Zr-O distance in sixfold coordination as reported by Shannon (1976). There are three additional O sites at a distance of 2.593 Å. Thus the corresponding coordination polyhedron could also be interpreted as a tri-capped trigonal prism.

The B site is located at the intersection of the threefold axis and the mirror plane ($z = 0.25$) in the center of the narrow, triangular channel. The nearest neighboring atoms are three symmetry equivalent O4 sites forming a regular triangle around B with a bonding distance 1.374 Å. Along [001] the sites located at 1/3, 2/3, z are alternately occupied by B and Zr, whereas the sequence in the laterally adjacent channel at 2/3, 1/3, z is inverted.

The Ca sites at 0, 0, 0 and 0, 0, 1/2 are located in the larger channel on the 6_3 screw axis. They are bonded to six symmetry-equivalent O atoms (O2 at 2.403 Å) of the octahedral framework. The Ca coordination may be described by an octahedron strongly flattened along **c** or by a distorted hexagon (Fig. 2). In this configuration the Ca site is laterally strongly restricted, but is relatively free to move along [001], normal to the coordination polygon. This is reflected in the strongly anisotropic atomic displacement parameters for Ca (Table 3, Fig. 2), which have a significantly larger component along [001]. One of the surprising results of the structure refinement was that the observed electron density (18.6 e/Å^3) at the Ca position was too low to be caused by complete Ca occupancy. The strong negative correlation between Ca and Na content observed in the LA-ICP-MS analyses of fragment no. 6b suggests a partial replacement of Ca by Na, which would explain the deficient electron density relative to a site occupied only by Ca. Actually, 19% Na substitution for Ca leads to the expected electron density of 18.3 e/Å^3, which is in excellent agreement with the refined value. The four-valent cation necessary for charge compensation is titanium, which replaces aluminum. Ti is distributed over two Al sites and contributes only with 2% to the Al occupancy. Thus this rather low concentration could not be resolved from the diffraction data.

The octahedral framework is composed of two types of AlO_6 octahedra with central sites Al1 and Al2. The bond angles in both polyhedra are distorted and show values between 77.52° and 102.57°, whereas the bonding distances vary between 1.821 and 2.082 Å (Table 5) and the averages are slightly shorter than the mean Al-O bonding distance of 1.935 Å (Shannon 1976). Octahedral distortions are triggered by the different ionic radii of Zr and B in the triangular channel (Fig. 3). The smaller B atom moves the connected octahedron vertices toward the center of the channel slightly reducing the aperture, whereas the larger Zr ion pushes the surrounding O atoms away from the center. This causes the undulating character of the edge-sharing bands of octahedra forming the framework.

In contrast, in the structurally related mineral fluoborite $B_3[Mg_9(F,OH)_9O_9]$ (e.g., Cámara and Ottolini 2000) the edge-sharing bands of Mg octahedra are straight because only B occupies the trigonal channels. Fluoroborite has for this reason **c**/3 periodicity relative to painite. Furthermore, the interior surface of the hexagonal channel in fluoborite is lined with F, OH and the channels are therefore empty. Jeremejevite $B_5[\square_3Al_6(OH)_3O_{15}]$ has three octahedral vacancies pfu replaced by three triangular

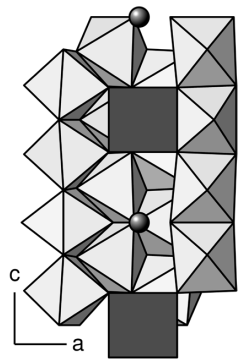

FIGURE 3. The edge-connected chains along [001] are affected by the size of the cation inside the channel. The small B atoms (spheres) move the connected vertices of octahedra toward the center of the channel, whereas the larger Zr atoms (dark squares, representing the prismatic coordination polyhedra) push the octahedra away from the center. This causes distortions in the octahedra and undulating characteristic of the framework chains.

TABLE 5. Selected interatomic distances (Å) for painite

Zr–O1	6×	2.1211(5)
Zr–O3	3×	2.5931(7)
Ca–O2	6×	2.4029(5)
Al1–O2		1.8489(5)
Al1–O3		1.8764(5)
Al1–O2		1.8904(5)
Al1–O1		1.9046(5)
Al1–O1		1.9128(5)
Al1–O4		2.0824(5)
Mean		1.919
Al2–O2	2×	1.8206(5)
Al2–O3		1.9051(7)
Al2–O1	2×	1.9472(5)
Al2–O4		2.0423(7)
Mean		1.914
B–O4	3×	1.3744(6)

BO_3 groups lining the wall of the hexagonal channels. Two additional BO_3 groups pfu plug the trigonal channels as in painite and fluoborite. In contrast to the suggestion by Moore and Araki (1976) all three minerals, painite (this study), fluoborite (e.g., Cámara and Ottolini 2000), and jeremejevite, (Rodellas et al. 1983; Sokolova et al. 1987) share the same space group $P6_3/m$.

ACKNOWLEDGMENTS

We thank R. Kampf and S. Krivovichev for their constructive reviews. This work was supported by the Swiss National Science Foundation (Grant 20-65084.01 to T.A., crystal chemistry of minerals), which is highly appreciated.

REFERENCES CITED

Cámara, F. and Ottolini, L. (2000) New data on the crystal-chemistry of fluoborite by means of SREF, SIMS and EMP analyses. American Mineralogist, 85, 103–107.

Claringbull-Gordon, F., Hey, M.H., and Payne, C.J. (1957) Painite, a new mineral from Mogok, Burma. Mineralogical Magazine, 31, 420–425.

Enraf-Nonius (1983) Structure determination package (SDP) (computer program), Enraf nonius, Delft, the Netherlands.

Golovastikov, N.I., Belova, J.N., and Belov, N.V. (1955) Crystal structure of jeremejevite. Zapiski Vsesoyuznogo Mineralogicheskogo Obschestva, 84, 405–414.

Günther, D., Frischknecht, R., and Heinrich, C.A. (1997) Capabilities of a 193 nm ArF excimer laser for LA-ICP-MS micro analysis of geological materials. Journal of Analytical Atomic Spectrometry, 12, 939–944.

Harlow, G.E. (2000) The Mogok Stone Tract, Myanmar: Minerals with complex prageneses. Proceedings of the 4th conference on "Minerals and Museums", Melbourne, Australia, 75.

Iyer, L.A.N. (1953) The geology and gem-stones of the Mogok Stone Tract, Burma. Memoirs of the Geological Survey of India, 82, 100.

Longerich, H.P., Jackson, S.E., and Günther, D. (1996) Laser ablation inductively coupled plasma mass spectrometry transient signal data acquisition and analyte concentration calculation. Journal of Analytical Atomic Spectrometry, 11, 899–904.

Moore, P.B. and Araki, T. (1976) Painite, $CaZrB[Al_9O_{18}]$: Its crystal structure and relation to jeremejevite, $B_5[BOX_3Al_6(OH)_3O_{15}]$, and fluoborite, $B_3[Mg_9(F,OH)_9O_9]$. American Mineralogist, 61, 88–94.

Peretti, A. (2003) New findings of painite. Contributions to Gemology, 2, 19–20.

Rodellas, C., Garcia-Blanco, S., and Vegas, A. (1983) Crystal structure refinement of jeremejevite ($Al_6B_5F_3O_{15}$). Zeitschrift für Kristallographie, 165, 255–260.

Shannon, R.D. (1976) Revised effective ionic radii and systematic studies of interatomic distances in halides and chalcogenides. Acta Crystallographica, A32, 751–767.

Sheldrick, G.M. (1997) SHELX-97 (computer program), University of Göttingen, Germany.

Shigley, J.E., Kampf, A.R., and Rossman, G.R. (1986) New data on painite. Mineralogical Magazine, 50, 267–270.

Sokolova, E.V., Egorov-Tismenko, Y.K., Kargal'tsev, S.V., Klyakhin, V.A., and Urnsov, V.S. (1987) Refinement of the crystal structure of synthetic fluorian jeremejevite $Al_6[BO_3]_5F_3$. Geologiya, 3, 82–84.

Webster, R. (1994) Gems, their sources, descriptions and identification, p. 1027. Butterworths, Sevenoaks, U.K.

MANUSCRIPT RECEIVED JULY 23, 2003
MANUSCRIPT ACCEPTED OCTOBER 21, 2003
MANUSCRIPT HANDLED BY PETER BURNS